JOURNAL OF CATALYSIS 57, 296–314 (1979)

Chemistry at Catalytic Surfaces

The SO_2 Oxidation on Noble Metals

C. G. VAYENAS* AND H. M. SALTSBURG

Department of Chemical Engineering, University of Rochester, Rochester, New York 14627

Received June 6, 1978; revised November 27, 1978

The high temperature solid electrolyte cell

$$\text{air}, M \,|ZrO_2(8\%\ Y_2O_3)|\, M, \text{air–}SO_2\text{–}SO_3,$$

where M is Pt, Ag, or Au, was used to monitor the oxygen activity on Pt, Ag, or Au catalyst films exposed to mixtures of O_2, SO_2, and SO_3 at temperatures above 400°C and 1 atm total pressure. One electrode functioned simultaneously as both electrode and catalyst. The open-circuit EMF of the cell reflected the oxygen activity on the working catalyst and simultaneously the steady-state chemical kinetics were observed. For Pt it was found that the surface oxygen activity generally does not equal the gas phase P_{O_2}, but is determined by P_{SO_2} or the P_{SO_3}/P_{SO_2} ratio, depending on the temperature and gas phase composition. These observations suggest that the rate-limiting step in the SO_2 oxidation on Pt is not generally the reaction between chemisorbed oxygen and gaseous SO_2, except at high temperatures and very low P_{SO_2}, but rather the desorption of a chemisorbed phase of SO_3 or the adsorption of oxygen, depending upon the temperature, P_{SO_2}, P_{SO_3}, and P_{O_2}.

The results with Au and Ag films show that chemisorbed SO_3 is also formed on these metals exposed to SO_2, O_2 mixtures. The values of surface oxygen activity compared to those obtained for Pt, provide an explanation for the weakly catalytic and noncatalytic properties of Au and Ag, respectively, for the SO_2 oxidation.

INTRODUCTION

A better understanding of heterogeneous catalytic reactions would be possible if the concentrations or the activities of the chemical species present on the catalyst surface during the reaction were known. Although various spectroscopic techniques have been employed to this end, limitations of either interpretation or applicability (e.g., inappropriate pressure ranges) have hampered progress. Bonding of elemental species is particularly difficult to assess; yet in the class of catalysts used for oxidation of organic or inorganic compounds, the role of chemisorbed oxygen must be of crucial importance. A technique utilizing an oxygen-ion-conducting solid electrolyte has been proposed (*1*) for the measurement of the thermodynamic oxygen activity on oxidation catalysts during reaction.

Accordingly, an investigation of the oxygen activity on a variety of oxidation catalysts has been undertaken with emphasis on those suitable for the oxidation of SO_2. The results of the study of SO_2 oxidation on noble metal catalyst films are described in the present communication.

Previous studies of the kinetics of the Pt-catalyzed SO_2 oxidation (*2–14*) are

* Present address: Department of Chemical Engineering, M.I.T., Cambridge, Massachusetts 02139.

0021-9517/79/050296-19$02.00/0
Copyright © 1979 by Academic Press, Inc.
All rights of reproduction in any form reserved.

generally in agreement concerning the first-order dependence of the reaction rate with respect to SO_2. However, various order numbers between 0 and 1 have been reported for O_2. The effect of SO_3 as a poison has been regularly observed, but various functional forms have been proposed to describe the rate dependence on P_{SO_3}. Most of the reported values of the activation energy fall between 11 and 15 kcal/mole. However, values as high as 23 kcal/mole or as low as 7 kcal/mole have been also reported (*7, 12*) under certain conditions. These results have been interpreted in terms of an equilibrium established between surface and gaseous oxygen coupled with gaseous or chemisorbed SO_2 attack on chemisorbed oxygen as the rate limiting step (*6, 8, 10*). Other workers have shown, however, that SO_3 is formed on the surface even at room temperature when SO_2 and oxygen coadsorb on Pt (*11, 15*) and have, therefore, suggested that desorption of SO_3 is rate limiting (*11*).

These interpretations can be examined more closely in light of the newly measured thermodynamic oxygen activity on the Pt surface during the reaction. In particular it will be shown that for Platinum: (1) Oxygen in the gas phase is not generally in equilibrium with chemisorbed oxygen, though there are conditions where equilibrium is reached; (2) there exists a form of SO_3 chemisorbed on Pt denoted by SO_3 (Pt) which acts as if it were a pure condensed phase, i.e., its chemical potential depends on temperature only; (3) the temperature and gas phase composition range of existence of SO_3(Pt) is limited and the limits can be defined; (4) in the region where SO_3(Pt) exists its desorption is the rate-limiting process and the rate of SO_2 oxidation is zero order with respect to O_2 and first order with respect to SO_2 changing to zero order for high P_{SO_2}; (5) at high temperatures and very low P_{SO_2}, the reaction between gaseous SO_2 and chemisorbed oxygen becomes rate limiting; therefore, the nature of the rate limiting step of the SO_2 oxidation on Pt is a function of both the temperature and the gas phase composition.

Since gold has been also reported to catalyze the SO_2 oxidation (*16, 17*), while Ag is inactive (*16*), it was of interest to extend these oxygen activity and kinetic measurements to these metals. It will be shown that the difference in the catalytic activity of Pt, Au, and Ag for the SO_2 oxidation is due to the different heats of chemisorption of SO_3 on these metals.

The basic technique for the measurement of oxygen activity in solids was first described by Wagner and Kiukkola (*18*). It utilizes a high temperature solid electrolyte cell with stabilized zirconia as the electrolyte. Yttria-stabilized zirconia exhibits essentially anionic conductivity over a very wide range of temperatures and partial pressures of oxygen (*19*). A similar cell has been used as an oxygen gauge in gas mixtures (*20, 21*) and high temperature stabilized zirconia fuel cells have also been investigated (*22, 23*). Stabilized zirconia cells have been also used as oxygen "pumps" to dissociate CO_2 and H_2O (*24*) and, more recently, NO (*25*). In the present study, attention was focused on the open-circuit EMF generated during the catalytic reaction when one of the electrodes serves as the catalyst and the other is exposed to a reference gas. C. Wagner had in fact proposed the use of stabilized zirconia cells to study the SO_2 oxidation on Pt in order to determine whether or not O_2 gas is in equilibrium with oxygen adsorbed on Pt during the reaction (*1*).

EXPERIMENTAL

The reactor cell used in the present study is shown in Fig. 1. The central part of the apparatus is a high-temperature stabilized zirconia cell consisting of the

solid electrolyte and two electrodes, one of them serving simultaneously as the catalyst under study. The 8% Y_2O_3 stabilized ZrO_2 tube, closed flat at one end, was sealed with a stainless steel cap/teflon gasket assembly at the other end. The cap had provision for introducing feed gas and removing effluent through $\frac{1}{8}$-in. stainless steel tubing, as well as provision for the introduction of a Pt, Ag, or Au wire, partly enclosed in a quartz tube, to make contact with the electrode on the inner base of the tube.

The base was platinized on both sides by painting with Engelhard Pt. No. 05 and baking at 700°C in air. This resulted in adherent, mechanically strong Pt electrodes. Similarly polycrystalline gold or silver film electrodes were deposited on both sides of the base of stabilized zirconia tubes using Engelhard Au No. 5154 and GC electronics Ag, respectively. Each cell was tested electrochemically at temperatures above 400°C using oxygen-inert gas mixtures of known P_{O_2} to insure its correct performance as an oxygen concentration cell before introduction of reactant SO_2. The outside film was exposed to ambient air and served as a reference electrode. An appropriately machined quartz base allowed for easy air access to the reference electrode and the top cap was clamped to the tube and the quartz base. A stainless steel baffle could be attached to the end of the inlet and outlet tubes inside the electrolyte tube in order to constrain the reactor volume to a practically isothermal region. The entire cell assembly was placed in a vertical tube furnace and the temperature was measured by means of an external thermocouple touching the outside wall of the electrolyte 2 mm from the reference electrode. The temperature of the cell was maintained by a controller following another thermocouple. At steady state the observed temperature differences were less than 3°C.

The dc potential difference across the cell was measured by a differential voltmeter having infinite input resistance at null. The maximum resistance of the electrolyte during measurements was of the order of a few hundred ohms.

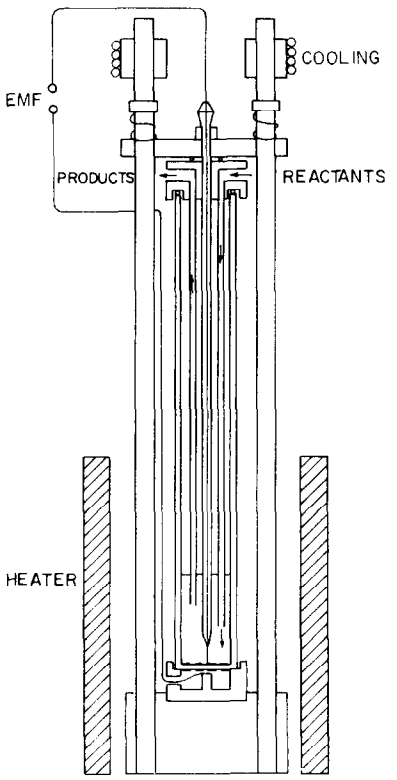

FIG. 1. Reactor cell configuration.

The analysis of the products was carried out by leaking a portion of the atmospheric pressure effluent stream through a differentially pumped system of orifices terminating in the high vacuum chamber of a mass spectrometer (Aerovac Monitor 712). During sampling the intermediate chamber pressure was typically 0.1 mm Hg and the spectrometer chamber pressure was 5×10^{-5} Torr (1 Torr = 133.3 N m^{-2}). Due to the length of connections the response of the mass spectrometer to a change in gas composition in the reactor was approximately 5 sec. Feed gases were prepared by premixing SO_2 and air or oxygen. The composition was determined

by controlling the flow rate of each gas but was also checked by direct mass spectrometric analysis of the feed stream utilizing a cell bypass system. Calibration was made using a SO_2–air mixture of known composition. The sensitivity of the mass spectrometric system permitted conversions at the 0.5% level to be detected.

In some experiments it was necessary to supply SO_3 in the feed gas. Accordingly, when needed, a preconverter consisting of a $\frac{1}{4}$-in. stainless steel tube containing 2 g of a commercial (Monsanto) promoted V_2O_5 catalyst was inserted in the flow system upstream of the electrolyte cell.

RESULTS

The SO_3 cracking pattern. In order to utilize the mass spectrometer, it was necessary to determine the cracking pattern of SO_3. Sulfur trioxide was produced catalytically using the preconverter and condensed in a brine-cooled loop that was inserted in the line between the reactor and the sampling system. The following relative intensities were observed for AMU 80, 64, and 48:

$$80:64:48 = 1:3.23:8.3.$$

This is in rough agreement with recently published data (*26*). These ratios together with the SO_2-cracking pattern, formed the basis for the determination of the SO_3/SO_2 ratio in the products.

Platinum: The open-circuit EMF and the oxygen activity. The open-circuit EMF of a solid electrolyte cell of the type utilized here is given by:

$$E = 1/4F[\mu_{O_2(Pt)\ \text{catalyst}} - \mu_{O_2(Pt)\ \text{reference}}], \quad (1)$$

where F is the Faraday constant and $\mu_{O_2(Pt)}$ is the chemical potential of oxygen adsorbed on the Pt electrodes. This expression is derived on the assumption that the electrolyte conducts by means of O^{2-} only and that the dominant exchange current reaction involves O^{2-} and adsorbed oxygen. The possibility of another dominant exchange current reaction will be discussed in the next section. Equation (1) includes as a limiting case the usual Nernst equation

$$E = \frac{RT}{4F} \ln \frac{P'_{O_2}}{P_{O_2}}, \quad (2)$$

which is valid only when no chemical reaction involving the gas phase proceeds at the electrode surface (*27*). In the general case it is the activity of oxygen adsorbed on the electrodes rather than the gas phase oxygen activity which determines the open-circuit EMF (*28*).

The chemical potential of oxygen at the reference electrode which is in contact with air ($P_{O_2} = 0.21$ atm) is given by

$$\mu_{O_2(Pt)\ \text{reference}} = \mu^\circ_{O_2(g)} + RT \ln (0.21), \quad (3)$$

where $\mu^\circ_{O_2(g)}$ the standard chemical potential of $O_2(g)$ at the temperature of interest.

The oxygen activity on the catalyst $a_{O_2(Pt)}$ is defined by a similar equation

$$\mu_{O_2(Pt)\ \text{catalyst}} = \mu^\circ_{O_2(g)} + RT \ln a_{O_2}(Pt). \quad (4)$$

Therefore, $a_{O_2(Pt)}$ expresses the partial pressure of gaseous oxygen that would be in equilibrium with oxygen on the Pt surface, if such an equilibrium were established. At temperatures of catalytic interest oxygen is well known to chemisorb dissociatively on platinum (*29*). The notation $a_{O_2(Pt)}$ does not imply molecular chemisorption but is simply a measure of the chemical potential of oxygen atoms chemisorbed on the surface if the partial pressure of oxygen in the gas phase were equal to $a_{O_2(Pt)}$ and no other gases were present in the gas phase. Combining (1), (2), and (4), $a_{O_2(Pt)}$ (atm) is given by

$$a_{O_2(Pt)} = 0.21 \exp\frac{4FE}{RT}. \quad (5)$$

If equilibrium is established between $O_2(g)$ and oxygen on the catalyst, then

$$a_{O_2(Pt)} = P_{O_2}.$$

This was verified experimentally over the temperature range 400 to 900°C by introducing into the reactor various O_2–He and O_2–Ar mixtures with P_{O_2} varying from 0.01 to 1 atm. Below 350°C significant delay was observed in obtaining steady state EMF values and no data were taken in this region.

Platinum: the open-circuit EMF under reaction conditions; the effect of SO_2. Introduction of a mixture of SO_2 and air into the previously air-equilibrated cell (EMF $= 0 \pm 1$ mV) resulted in an immediate decrease in the open-circuit EMF by several hundred millivolts. This indicates that $a_{O_2(Pt)}$ has decreased from 0.21 atm to a value in the range of 10^{-6}, i.e., five orders of magnitude lower than P_{O_2} in the gas phase in contact with the catalyst. At the same time the analysis of the effluent stream showed that conversion to SO_3 was occurring but the conversion was not nearly enough to measurably deplete the gaseous oxygen in the cell. Upon removal of the SO_2 component, equilibrium between gaseous O_2 and oxygen on Pt was rapidly reestablished indicating the reversibility of the process.

The value of $a_{O_2(Pt)}$ was measured over

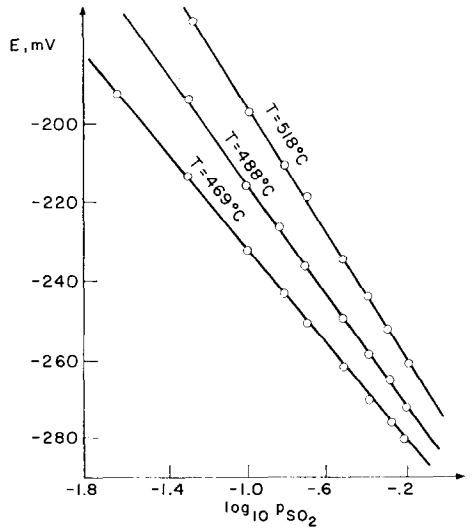

FIG. 2. Open-circuit EMF during reaction.

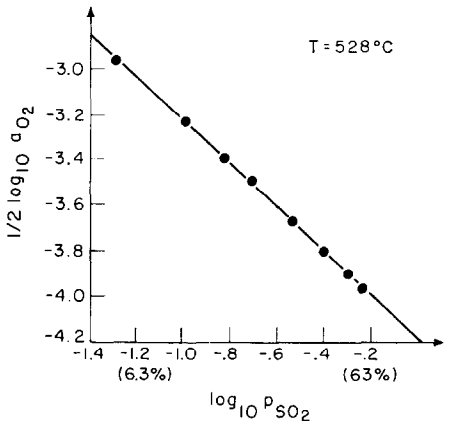

FIG. 3. Reciprocal relationship between P_{SO_2} and $a_{O_2(Pt)}^{1/2}$.

the temperature range 400–850°C with the gas phase partial pressure of SO_2 varying in the feed stream between 0.015 and 0.6 atm. It was found that over a wide temperature and composition range, $a_{O_2(Pt)}$ is a function of P_{SO_2} and T only. Typical examples are illustrated in Fig. 2. Analysis of the data in this range revealed the existence of a reciprocal relationship between P_{SO_2} and $a_{O_2(Pt)}$ (Fig. 3) and further that

$$P_{SO_2} \times a_{O_2(Pt)}^{1/2} = K_{Pt}(T), \qquad (6)$$

where K_{Pt} is a function of T only (Fig. 4),

$$\ln K_{Pt} = 13.6\ (\pm 1.0) - 17{,}600\ (\pm 1000)(1/T). \qquad (7)$$

Equations (6) and (7) suggest that increasing the temperature, at constant P_{SO_2}, will result in an increase in $a_{O_2(Pt)}$. It was found that when the temperature is reached where $a_{O_2(Pt)} = P_{O_2}$ then with further increase in temperature, $a_{O_2(Pt)}$ follows the P_{O_2} value and does not satisfy Eq. (6) any longer (Fig. 5). Therefore, the range where Eq. (6) is satisfied is, in part, limited to a range defined by

$$P_{SO_2} \times P_{O_2}^{1/2} > K_{Pt}. \qquad (8)$$

It was also found that as long as Eq. (6)

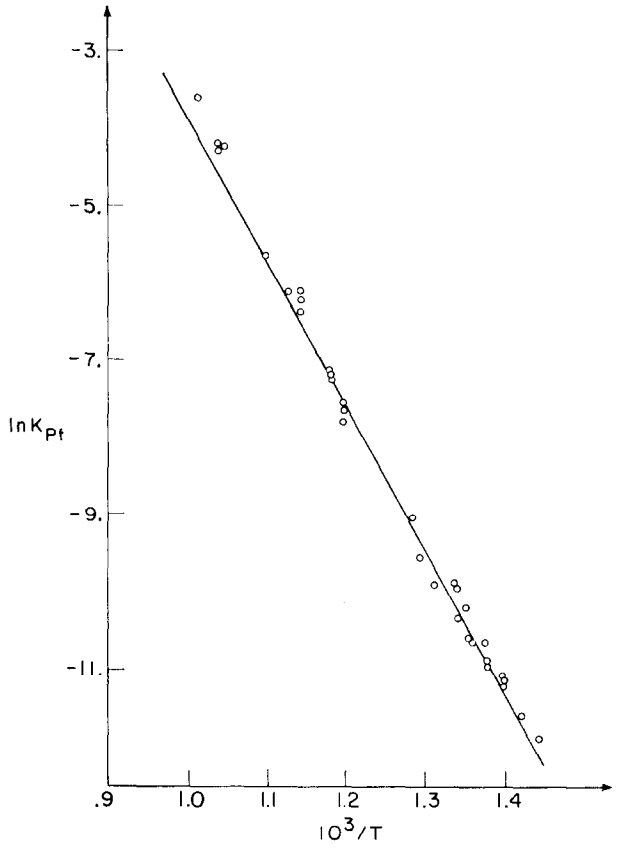

FIG. 4. Temperature dependence of K_{Pt}.

was satisfied, the value of P_{SO_3} in the cell operating as a CSTR reactor would not exceed a value defined by $K_P K_{Pt}$ at this temperature:

$$P_{SO_3} < K_P K_{Pt}, \tag{9}$$

where K_P is the equilibrium constant for the gas phase equilibrium

$$SO_2(g) + \tfrac{1}{2}O_2(g) = SO_3(g). \tag{10}$$

This was valid (within the error limits of $K_P K_{Pt}$) even for $P_{SO_2} = 0.6$ atm (Fig. 6).

By using the V_2O_5 catalytic preconverter in order to introduce SO_3 into the feed stream of the CSTR cell reactor, it was found that as long as P_{SO_3} in the CSTR is below $K_P K_{Pt}$, Eq. (6) is satisfied.

However, when $P_{SO_3} > K_P K_{Pt}$ then a new equilibrium is established:

$$\frac{P_{SO_3}}{P_{SO_2} \times a_{O_2(Pt)}^{1/2}} = K_P. \tag{11}$$

This is shown in Fig. 7. It should be noted that $a_{O_2(Pt)}$ is still well below P_{O_2} and hence gas phase equilibrium is not established.

No dependence of $a_{O_2(Pt)}$ on the total flow rate (varying between 20 and 160 ml/min) or on the thickness of the Pt film (roughly between 3 and 8 μm) was observed. The surface oxygen activity was a function of the gas phase partial pressures and the temperature only.

Oxidation kinetics. Perfect mixing was assumed to occur in the gas phase in the reactor cell and the rate was calculated

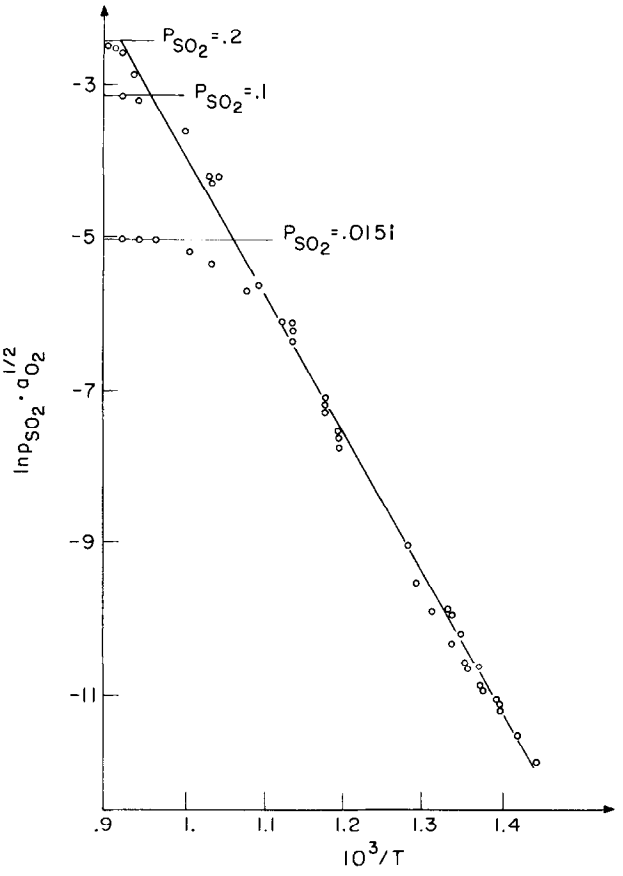

FIG. 5. Temperature dependence of $P_{SO_2} \times a_{O_2(Pt)}^{1/2}$ with three different SO_2–air mixtures at 1 atm total pressure including range where $a_{O_2(Pt)} = P_{O_2}$.

from the appropriate mass balance

$$r = F'[XSO_3(\text{effluent}) - XSO_3(\text{feed})], \tag{12}$$

where F' is the total molar flow rate and X the mole fraction of SO_3. Most of the kinetic data were taken between 400 and 600°C and without the use of the pre-converter, therefore, under conditions where Eq. (6) was satisfied. The zirconia tube itself was not capable of catalyzing the oxidation reaction to any detectable degree in this temperature range. The feed stream impinged on the Pt film with velocities of the order 20 cm/sec to avoid mass transfer limitations. No dependence of the rate on the total flow rate was observed, and this, in conjunction with the flow rate independent surface oxygen activity, shows that the low values of the surface oxygen activity are not the result of a diffusion limited reaction process. Very low surface oxygen activities were also observed on other metals (*30*), including Ag which was inactive for the SO_2 oxidation, again ruling out a transport limited process.

The observed rate is exhibited in Fig. 8 as a function of P_{SO_2} for two temperatures. The rate is first order with respect to SO_2 for P_{SO_2} below approximately 0.3 atm, but above that the rate tends to become almost independent of P_{SO_2}. No detectable dependence of the rate on P_{O_2} was found

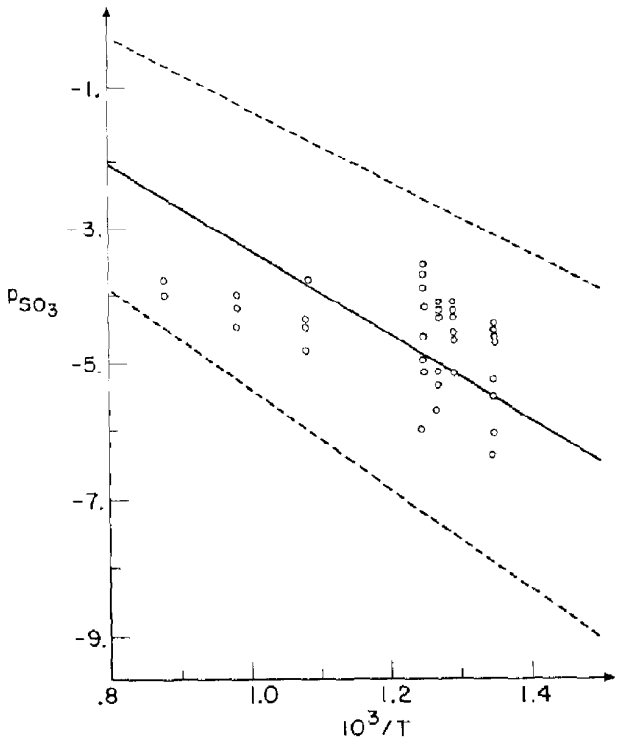

FIG. 6. Comparison of maximum measured P_{SO_3} values (without a preconverter) with the electrochemically predicted maximum P_{SO_3} (solid line). Dashed lines are error limits of predicted maximum P_{SO_3}.

within the limits 0.08 atm $< P_{O_2} <$ 0.2 atm. The activation energy obtained from the linear rate vs P_{SO_2} region was found to be 11 kcal/mol (Fig. 9). However, practically the same value was obtained from the values of the rate coefficient at

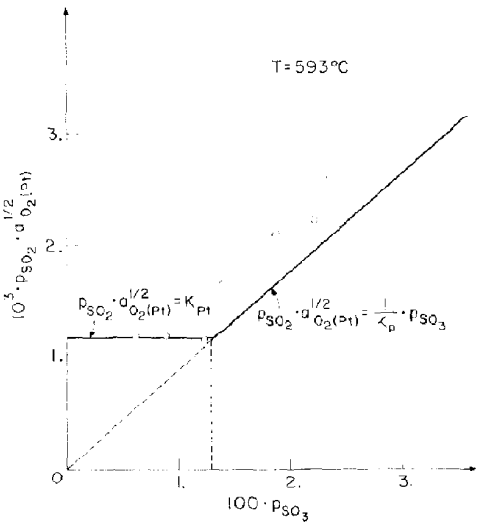

FIG. 7. Transition of surface equilibrium from $P_{SO_3} < K_P K_{Pt}$ to $P_{SO_3} > K_P K_{Pt}$.

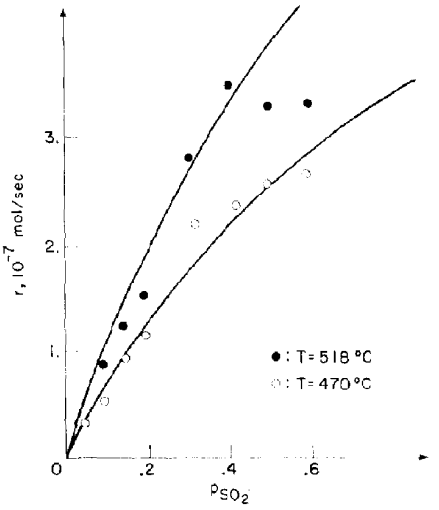

FIG. 8. Rate of oxidation as function of P_{SO_2} at T = 470 and 518°C. No preconverter. Solid lines from Eq. (29).

high P_{SO_2}, where the rate is independent of P_{SO_2}.

Silver: EMF under reaction conditions. The predicted performance of the oxygen concentration cell was verified by introducing various O_2–He and O_2–Ar mixtures of known P_{O_2} in the reactor and obtaining open-circuit EMF values in agreement with Eq. (2) within 1 mV.

Introduction of SO_2–air mixtures in the previously air-equilibrated reactor cell ($E = 0 \pm 1$ mV) resulted in the appearance of large negative voltages ($E \sim -350$ mV), corresponding to $a_{O_2(Ag)} \sim 10^{-10}$ atm. As with Pt films, $a_{O_2(Ag)}$ varies only with P_{SO_2} and T and $a_{O_2(Ag)} \ll P_{O_2}$. The removal of SO_2 from the feed stream restored the system to the oxygen equilibrium value but the process was slower than the corresponding on Pt.

There was no indication of any catalytic conversion of SO_2 over the temperature range 400 to 550°C within the limits of detection (>0.5% conversion).

The open-circuit EMF was measured simultaneously with P_{SO_2} varying from 0.015 atm to 0.6 atm, the balance being air. The functional dependence of surface oxygen activity on P_{SO_2} and T was similar to that found with Pt:

$$P_{SO_2} \cdot a_{O_2(Ag)}^{1/2} = K_{Ag}(T), \qquad (13)$$

$$\ln K_{Ag}(T) = 18.4 - 24{,}000/T. \qquad (14)$$

At temperatures of catalytic interest $K_{Ag}(T)$ is significantly lower than the corresponding parameter $K_{Pt}(T)$ obtained with Pt catalysts.

Gold: EMF under reaction conditions and oxidation kinetics. The correct performance of the cell at temperatures above 400°C was verified exactly as in the case of silver electrodes. However, establishment of steady state open-circuit EMF values satisfying Eq. (2) was slower with gold electrodes (a few minutes at 400°C) than with silver or platinum electrodes. Upon introduction of SO_2–air mixtures in the cell reactor, the EMF of the previously air-equilibrated cell again dropped to a large negative value (~ -250 mV), implying $a_{O_2(Au)} \sim 10^{-7}$ atm. Conversion to SO_3 was observed but to a lesser extent than with Pt under the same conditions. A limited study of the kinetics indicated a practically first-order dependence of the rate on P_{SO_2}. Removal of the SO_2 component restored the oxygen equilibrium.

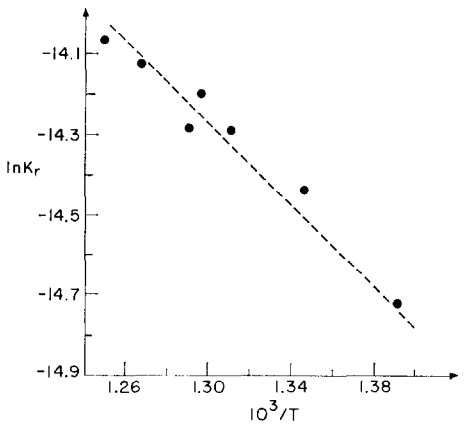

FIG. 9. Temperature dependence of the rate for linear range of rate vs P_{SO_2} (K_R = rate/P_{SO_2}).

The surface oxygen activity was studied at temperatures between 400 and 600°C. It was found that $a_{O_2(Au)}$ is a function of P_{SO_2} and T. However, the simple reciprocal relationship between P_{SO_2} and a_{O_2} observed with Ag and Pt was not valid at the lower temperatures studied; the decrease in $a_{O_2(Au)}$ with increasing P_{SO_2} at constant T is more pronounced than the one described by an expression of the form $P_{SO_2} \cdot a_{O_2(Au)}^{1/2} = K_{Au}$. At these lower temperatures the product $P_{SO_2} \cdot a_{O_2(Au)}^{1/2}$ is not constant for constant T, although the values of $K_P \cdot P_{SO_2} \cdot a_{O_2(Au)}^{1/2}$ (K_P is the gas phase equilibrium constant) fall between the corresponding values for Pt and Ag at the same temperature (Figs. 10, 11). The surface oxygen activity was found to be better approximated by an expression

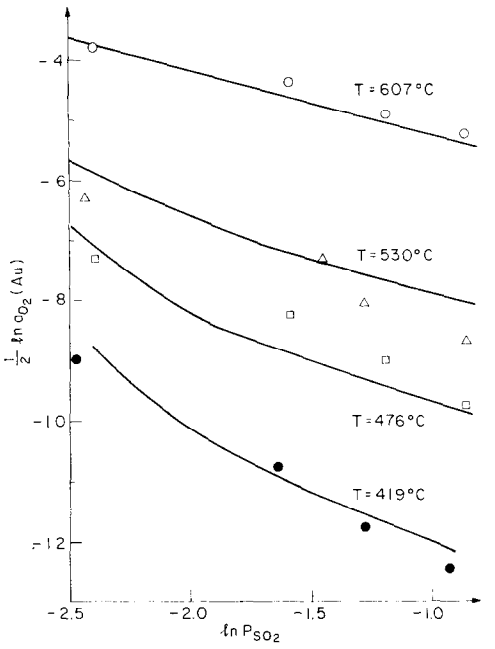

FIG. 10. Surface oxygen activity on gold vs P_{SO_2}. Solid lines obtained from Eqs. (15)–(17).

of the form

$$P_{SO_2} \cdot a_{O_2(Au)}^{1/2} = K_{Au}[1 + K_O a_{O_2(Au)}^{1/2}], \quad (15)$$

with

$$\ln K_{Au} = 17.1 - 21{,}000/T \quad (16)$$

and

$$\ln K_O = -23.8 + 24{,}000/T, \quad (17)$$

with a greater uncertainty for K_O. At the higher temperatures studied the product $P_{SO_2} \cdot a_{O_2(Au)}^{1/2}$ becomes practically constant and equal to K_{Au}.

DISCUSSION

SO_2 oxidation on Pt: the equilibrium constant K_{Pt}. The very low values of $a_{O_2(Pt)}$ compared to P_{O_2} during the reaction in the region where Eq. (6) is satisfied show that gaseous and chemisorbed oxygen are not in equilibrium. Equation (6), however, is suggestive of another equilibrium between $SO_2(g)$ and chemisorbed oxygen. The simplest such equilibrium which satisfied the stoichiometry represented by Eq. (6) is

$$SO_2(g) + O(Pt) \rightleftarrows SO_3(Pt). \quad (18)$$

The product of this equilibrium step could not be $SO_3(g)$, since a constant $P_{SO_2} \times a_{O_2(Pt)}^{1/2}$ value would imply a constant P_{SO_3}, which is not what was observed. However, when equilibrium (18) obtains, it implies, in view of Eq. (6) that $SO_3(Pt)$ has an activity which is a function only of temperature, independent of concentration of surface SO_3. Such a property is characteristic of a pure "condensed" phase. This discussion can be made quantitative and the chemical potential of $SO_3(Pt)$ relative to $SO_3(g)$ can be computed.

When equilibrium (18) obtains, then

$$\mu_{SO_2} + \tfrac{1}{2}\mu_{O_2(Pt)} = \mu_{SO_3(Pt)}.$$

Taking into account Eq. (4) and using gaseous standard states one obtains

$$\mu^\circ_{SO_2(g)} + \tfrac{1}{2}\mu^\circ_{O_2(g)} + RT \ln P_{SO_2} a_{O_2(Pt)}^{1/2} = \mu_{SO_3(Pt)}.$$

Combining with Eq. (6),

$$\mu_{SO_3(Pt)} = \mu^\circ_{SO_2(g)} + \tfrac{1}{2}\mu^\circ_{O_2(g)} + RT \ln K_{Pt}. \quad (19)$$

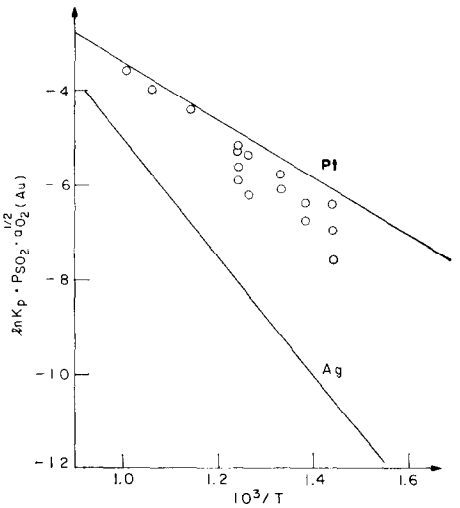

FIG. 11. Measured values of $K_P \cdot P_{SO_2} \cdot a_{O_2(Au)}^{1/2}$ compared to $K_P K_{Pt}$ and $K_P K_{Ag}$.

Since all the terms on the right of Eq. (19) are functions only of T, $\mu_{SO_3(Pt)}$ is only a function of T, and since

$$\Delta G^\circ_T = -RT \ln K_P = \mu^\circ_{SO_3(g)} - \mu^\circ_{SO_2(g)} - \tfrac{1}{2}\mu^\circ_{O_2(g)}, \quad (20)$$

one can compute $\mu_{SO_3(Pt)}$ relative to the gaseous SO_3 standard state

$$\mu_{SO_3(Pt)} = \mu^\circ_{SO_3(g)} + RT \ln K_P K_{Pt}. \quad (21)$$

Inserting the appropriate numerical values

$$\mu_{SO_3(Pt)} - \mu^\circ_{SO_3(g)} = (2.8 \pm 1.)RT - (6200 \pm 1000)R, \quad (22)$$

where $R = 8.31$ J K^{-1} mol^{-1} and T in K. The last equation permits calculation of the "vapor pressure" of chemisorbed SO_3(Pt), i.e., of the partial pressure of SO_3(g) that would be in equilibrium with SO_3(Pt) if such an equilibrium were established:

$$\ln P_{SO_3}\,(\text{atm}) = \ln K_{Pt}K_P = 2.8(\pm 1.) - [6200(\pm 1000)/T]. \quad (23)$$

Therefore, the heat of chemisorption of SO_3(Pt) can be calculated and is found to be 12.3 ($\pm$2.) kcal/mol in very good agreement with the value of 12.1 kcal/mol reported by Hurt (*8*). This is also very close to the value of the activation energy (11 kcal/mol) observed in the region of existence of SO_3(Pt). The origin of this agreement is discussed below.

The stability of SO_3(Pt). Examination of the "vapor pressure" expression for SO_3(Pt) shows that unless $a_{O_2(Pt)} = P_{O_2}$ the gaseous equilibrium value of P_{SO_3} will not be achieved at any of the low temperatures of catalytic interest. The phase SO_3(Pt) must therefore have limited stability and at least one of the stability limits must be reached on the approach to gas phase equilibrium. This is in nice agreement with the experimental results since SO_3(Pt) exists only in the region where Eq. (6) is satisfied. This region is defined by the two inequalities (8) and (9), i.e., $P_{SO_2} \times P_{O_2}^{1/2} > K_{Pt}$ and $P_{SO_3} < K_P K_{Pt}$. Both inequalities must be satisfied for SO_3(Pt) to exist. The region of existence of SO_3(Pt) in SO_2–air mixtures at 1 atm total pressure is shown in Fig. 12. As little as 100 ppm SO_2 in air are sufficient to form SO_3(Pt) at 500°C.

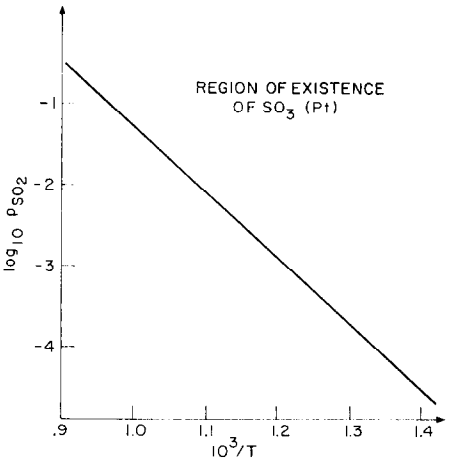

FIG. 12. Region of stability of SO_3(Pt) in SO_2–air mixtures at 1 atm; $P_{SO_3} < K_P K_{Pt}$.

When equilibrium in the gas phase is established, i.e.,

$$\frac{P_{SO_3}}{P_{SO_2} \times P_{O_2}^{1/2}} = K_P, \quad (24)$$

then SO_3(Pt) does not generally exist, because if $P_{SO_3} > K_P K_{Pt}$ then Eq. (9) is not satisfied, and if $P_{SO_3} < K_P K_{Pt}$, it follows that $P_{SO_2} \times P_{O_2}^{1/2} < K_{Pt}$ and Eq. (8) is not satisfied. In a closed system containing SO_2, SO_3, and O_2 in contact with Pt and held at constant temperature and total pressure, when equilibrium in the gas phase is ultimately established, SO_3(Pt) will exist only in the exceptional case where $P_{SO_3} = K_P K_{Pt}$.

That SO_3(Pt) cannot be formed when $P_{SO_2} \times P_{O_2}^{1/2} < K_{Pt}$ can be easily understood since in this case $\mu_{SO_2(g)} + \frac{1}{2}\mu_{O_2(g)} < \mu_{SO_3(Pt)}$. The reason SO_3(Pt) is destroyed and $a_{O_2(Pt)}$ is determined by the P_{SO_3}/P_{SO_2} ratio as soon as P_{SO_3} exceeds $K_P K_{Pt}$ is not so obvious from a thermodynamic

point of view. However, if $P_{SO_3} > K_P K_{Pt}$ and $P_{SO_3} \times a_{O_2}^{1/2} = K_{Pt}$, then $\mu_{SO_3(g)} > \mu_{SO_3(Pt)}$ and $\mu_{O_2(g)} > \mu_{O_2(Pt)}$, and therefore there would be a tendency for additional adsorption of both SO_3 and oxygen on the finite surface area of the catalyst. It is probable that this accumulation of SO_3 on the surface, which occurs as soon as $P_{SO_3} > K_P K_{Pt}$, results in a structural change of chemisorbed SO_3 and in the destruction of SO_3(Pt).

Consequently, to the above discussion if a mixture of pure SO_2 and O_2 is introduced in a closed vessel containing Pt and held at a uniform temperature T and constant total pressure P, SO_3(Pt) will be originally formed, provided $P_{SO_2} \times P_{O_2}^{1/2} > K_{Pt}$, but once the saturation "vapor pressure" is reached (i.e., $P_{SO_3} = K_P K_{Pt}$) the process will come to a temporary halt. However, any fluctuation in temperature or concentration will produce a "supersaturated" SO_3 vapor which in turn destroys SO_3(Pt), allowing the reaction to proceed until P_{SO_3} reaches the value characteristic of the gas phase K_P. If the original SO_2, O_2 mixture is such that $P_{SO_2} \times P_{O_2}^{1/2} < K_{Pt}$, then SO_3(Pt) will not be formed during the approach to gas phase equilibrium.

One can summarize the stability limits for SO_3(Pt) as follows:

Region 1.	$P_{SO_2} \times P_{O_2}^{1/2} < K_{Pt}$	SO_3(Pt) is not formed, $a_{O_2(Pt)} = P_{O_2}$.
Region 2.	$P_{SO_2} \times P_{O_2}^{1/2} > K_{Pt}$ $P_{SO_3} < K_P K_{Pt}$	SO_3(Pt) is stable, $P_{SO_2} \times a_{O_2}^{1/2} = K_{Pt}$, $a_{O_2(Pt)} < P_{O_2}$.
Region 3.	$P_{SO_2} \times P_{O_2}^{1/2} > K_{Pt}$ $P_{SO_3} > K_P K_{Pt}$	SO_3(Pt) is not formed, $P_{SO_3}/P_{SO_2} \times a_{O_2(Pt)}^{1/2} = K_P$, $a_{O_2(Pt)} < P_{O_2}$.

The nature of SO_3(Pt). Since the available information is strictly thermodynamic, one cannot describe the structure of this phase in detail, other than speculatively, but comparison with the properties of bulk condensed phase SO_3 is interesting. There are three different phases of solid SO_3, all polymeric (*31*). These include two- and three-dimensional linear polymers (α and β) stabilized by impurities and a ring structure S_3O_9 (*31*).

The liquid appears to be a mixture of SO_3 and S_3O_9 rings. The heat of vaporization of liquid SO_3 is 10.2 kcal/mol and the heats of sublimation of solid SO_3 are 13.2, 13.8, and 16.1 kcal/mol, respectively, for γ, β, and α forms, close to the derived value of 12.3 kcal/mol for the heat of adsorption of SO_3(Pt). The calculated entropy of desorption of SO_3(Pt) is 5.4 $\pm$ 2. cal/mol K [Eq. (23)]. Such low values are possible only if a large configurational entropy is associated with the adsorbed phase. The ability of SO_3 to form linear polymers suggests that SO_3(Pt) may be just such a set of polymeric chains formed by bonding along the surface. Such structures may be the high pressure analog of the islands of chemisorbed species observed in LEED studies of chemisorption (*32*) and also invoked to explain the details of the formic acid decomposition on Ni (*33*). Due to the difficulties of forming and maintaining SO_3(Pt) under vacuum conditions [Eq. (8)], electron spectroscopic and diffraction techniques may not prove useful to examine this structure. Infrared studies, however, should be capable of providing useful additional information.

The reaction "mechanism" on platinum. Most previous studies of this reaction had

assumed equilibration between gaseous and chemisorbed oxygen (*6, 8*) with a rate limiting step involving the reaction of gaseous or adsorbed SO_2 with chemisorbed oxygen. The direct measurement of the surface oxygen activity shows that the oxygen equilibrium is not established in the presence of SO_2, except in Region 1. In Region 2 Eq. (6) implies that the interaction between $SO_2(g)$ and chemisorbed oxygen is an equilibrium process and, therefore, cannot be rate limiting. Similarly in Region 3, Eq. (11) implies that equilibrium is established for the reaction

$$SO_2(g) + O(Pt) \rightleftarrows SO_3(g), \qquad (25)$$

which again rules out the reaction step between $SO_2(g)$ and chemisorbed oxygen as a rate limiting step.

In Region 2, equilibrium (18) is established and the kinetic data must be explained, taking into account the existence of $SO_3(Pt)$. These data include the form of the rate dependence on P_{SO_3} (Fig. 8), the rate independence on P_{O_2}, and an activation energy of 11 kcal/mol. These observations are consistent with a mechanism involving the desorption of $SO_3(Pt)$ as a rate-limiting process by means of the following steps:

$$\begin{aligned} SO_2(g) + O(Pt) &\rightleftarrows SO_3(Pt), \\ SO_3(Pt) &\rightarrow SO_3(g), \qquad \text{R.L.S.}, \\ \tfrac{1}{2}O_2(g) &\rightarrow O(Pt). \end{aligned}$$

That SO_3 desorption is rate limiting has been concluded by several previous investigators who showed that the rate of SO_2 oxidation parallels the rate of SO_3 desorption from several catalysts, including Pt on silica and Pt on alumina, and that SO_3 is formed on the surface even at room temperature when SO_2 and O_2 coadsorb on Pt (*11*). It has been shown also that at room temperature the ratio of the amount of oxygen chemisorbed on Pt black to the amount of SO_2 chemisorbed on oxygen-covered Pt black is approximately 0.5 (*15*).

The proposed mechanism utilizing the existence and stability limits of $SO_3(Pt)$ also provides an alternative explanation for the SO_3 poisoning effect in Region 2. In contrast to the usual discussion of site blocking, the existence of $SO_3(Pt)$ implies the development of a reversible poisoning, the rate of the forward reaction being limited by the approach of the system to the saturation vapor pressure of $SO_3(Pt)$. As P_{SO_3} approaches $K_P K_{Pt}$, the net rate will tend to be zero as long as $SO_3(Pt)$ still exists, since the rate of SO_3 readsorption will approach the rate of $SO_3(Pt)$ desorption. In a typical CSTR reactor with a feed of only SO_2 and air, P_{SO_3} cannot build up except at very low flow rates. The upper limit of P_{SO_3} observed in the present study (without the use of the preconverter) satisfies this vapor pressure requirement (Fig. 6).

In Region 3, since equilibrium is established for the step

$$SO_2(g) + O(Pt) \rightleftarrows SO_3(g), \qquad (25)$$

the remaining step

$$\tfrac{1}{2}O_2(g) \rightarrow O(Pt)$$

must control the rate. Under such conditions chemisorbed SO_3 hinders the rate-limiting oxygen chemisorption and gives rise again to SO_3 self-poisoning. It seems therefore that the nature of the SO_3 poisoning effect is different depending upon whether $P_{SO_3} < K_P K_{Pt}$ or $P_{SO_3} > K_P K_{Pt}$. Although sufficient kinetic data were not available to confirm this point, it seems likely that the vapor pressure curve of $SO_3(Pt)$ represents a boundary for the reaction mechanism.

In a tubular flow reactor and particularly under nonisothermal conditions P_{SO_3} can easily exceed $K_P K_{Pt}$. When this happens, one part of the reactor close to the entrance, operates under the conditions of

Region 2 while the rest of the reactor operates under the conditions of Region 3.

The present study also suggests that a UHV study of the oxidation of SO_2 on Pt at the temperatures of catalytic interest would not reveal the relevant kinetics and structures appropriate to atmospheric pressure conditions, since the inequality $P_{SO_2} \times P_{O_2}^{1/2} > K_{Pt}$ would not be satisfied (Fig. 12). Under such conditions (Region 1) the reaction between SO_2 and chemisorbed oxygen would be rate controlling. In light of the different kinetic behavior (i.e., different rate limiting steps) in each of the three regions, it is not surprising that a variety of complex rate expressions have been proposed to describe the kinetics of the SO_2 oxidation on Pt.

Quantitative oxidation kinetics on platinum. An interpretation of Eq. (6) in terms of surface coverages as well as its implications for the kinetics of the reaction in Region 2 can be provided by the following model.

Considering the equilibrium step

$$SO_2(g) + O(Pt) \rightleftarrows SO_3(Pt) \qquad (18)$$

and assuming mass action kinetics one obtains

$$K \times P_{SO_2} \times \Theta_O = K\Theta_{SO_3}, \qquad (26)$$

where Θ_O, Θ_{SO_3} are the surface coverages of oxygen and SO_3, respectively, and K, K' are temperature-dependent coefficients that satisfy

$$\frac{K'}{K} = \exp\frac{\Delta G^\circ_R}{RT}, \qquad (27)$$

where ΔG°_R refers to the equilibrium reaction step. By further assuming $\Theta_{SO_3} + \Theta_O \simeq 1$, which is quite reasonable at these relatively high pressures, one obtains from (26)

$$P_{SO_2} \times \frac{\Theta_O}{1 - \Theta_O} = \frac{K'}{K}. \qquad (28)$$

Comparing (28) and (6) it follows that

$$a_{O_2(Pt)}^{1/2} = \frac{\Theta_O}{1 - \Theta_O} \times \frac{K_{Pt}}{K'/K}. \qquad (29)$$

Since $a_{O_2(Pt)}$ expresses the partial pressure of gaseous oxygen that would be in equilibrium with chemisorbed oxygen if such an equilibrium were established, Eq. (29) shows that oxygen chemisorption can be described at least approximately by a simple Langmuir expression:

$$a_{O_2(Pt)}^{1/2} = \frac{\Theta_O}{(1 - \Theta_O)K_O}, \qquad (30)$$

where K_O is the adsorption coefficient of oxygen on platinum, since clearly from (19) and (27)

$$K_O = \frac{K'}{K} K_{Pt}. \qquad (31)$$

Alternatively, from (28) one could have predicted that for constant T the product $P_{SO_2} \times a_{O_2}^{1/2}{}_{(Pt)}$ would be constant assuming that oxygen chemisorption on platinum at these temperatures and pressures can be treated approximately by a Langmuir model. This does not imply that this is the only model that can explain Eq. (6) but it is the simplest.

Since SO_3 desorption is rate limiting and assuming the SO_3 readsorption term to be negligible, the rate of the overall reaction can be written as

$$r = C \times \Theta_{SO_3} = C \times (1 - \Theta_O) \qquad (32)$$

and using (28),

$$r = C \frac{P_{SO_2}}{K_{Pt}K_O + P_{SO_2}}. \qquad (33)$$

On the assumption that SO_3 adsorption is nonactivated, C can be written as $C^*K_PK_{Pt}$, where C^* is temperature independent,

therefore

$$r = C^*K_PK_{Pt} \times \frac{P_{SO_2}}{K_{Pt}K_O + P_{SO_2}}. \quad (34)$$

This expression would explain the observed kinetic behavior and also the observed activation energy of 11 kcal/mol if the product $K_{Pt}K_O$ is a weak function of T. If one assumes a value of 68 kcal/mol for the heat of chemisorption of O_2 on Pt (*29*), then $K_O = K^*_O \exp(+34{,}000/RT)$, where K^*_O is temperature independent. Since $K_{Pt} = 7.7 \times 10^5 \times \exp(-34{,}500/RT)$, it follows that the product $K_{Pt}K_O$ is essentially temperature independent. This also implies that Θ_{SO_3} depends very little on temperature for given P_{SO_2}. From the kinetic data obtained in this study the value of $K_{Pt}K_O$ is approximately 0.4 atm in the region between 400 and 600°C. Alternatively, the surface reaction step is practically athermal (−600 cal/mol exothermic), which could have been directly derived on the basis of the values of 68 and 12.1 kcal/mol for the heat of chemisorption of O_2 and SO_3 on Pt, respectively. Equation (34) describes the kinetic data shown in Fig. 8 as well as those of Lewis and Ries (*2*) which were obtained at such low P_{SO_2} and P_{SO_3} that the first-order P_{SO_2} dependence was observed and $K_PK_{Pt} \gg P_{SO_3}$ was satisfied. The preceding analysis is valid as long as P_{SO_3} is not very close to K_PK_{Pt} in which case the SO_3 readsorption term should be included.

For P_{SO_3} exceeding K_PK_{Pt} (Region 3), in which case equilibrium is established for the step

$$SO_2(g) + O(Pt) \rightleftarrows SO_3(g),$$

equilibrium must also be established between surface and gaseous SO_3. The experimentally observed relationship

$$\frac{P_{SO_3}}{P_{SO_2} \times a_{O_2(Pt)}^{1/2}} = K_P \quad (11)$$

is accounted for by the previous model by

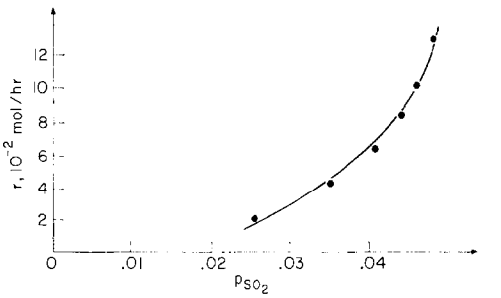

FIG. 13. Rate vs P_{SO_2} for $P_{SO_3} + P_{SO_3} = 0.068$ atm at 480°C (*34*) compared with Eq. (37). $K_{Pt} \times K_0 = 0.4$ atm and $K_PK_{Pt} = 4.6 \times 10^{-3}$ atm at 480°C.

inclusion of the equilibrium between gas phase and chemisorbed SO_3. One has

$$\Theta_O = \frac{K_O a_{O_2(Pt)}^{1/2}}{1 + K_O a_{O_2(Pt)}^{1/2} + K_{SO_3}P_{SO_3}},$$

$$\Theta_{SO_3} = \frac{K_{SO_3}P_{SO_3}}{1 + K_O a_{O_2(Pt)}^{1/2} + K_{SO_3}P_{SO_3}}, \quad (35)$$

where K_O, K_{SO_3} are adsorption coefficients of O_2 and SO_3, respectively. Substituting into (26) and using (31)

$$\frac{P_{SO_3}}{P_{SO_2}a_{O_2}^{1/2}} = \frac{K_O}{K_{SO_3}(K'/K)} = \frac{1}{K_{Pt}K_{SO_3}}. \quad (36)$$

Comparing with (11) one obtains $K_{SO_3}^{-1} = K_PK_{Pt}$. This implies that the heat of chemisorption of SO_3 is 12.3 kcal/mol in this region, too. Since in this region oxygen chemisorption is rate limiting, the rate of the forward reaction can be written as

$$r = C'P_{O_2}^{1/2}(1 - \Theta_O - \Theta_{SO_3}) = C'K_PK_{Pt} \times \frac{P_{SO_2} \times P_{O_2}^{1/2}}{K_PK_{Pt}P_{SO_2} + P_{SO_3}(P_{SO_2} + K_{Pt}K_O)}. \quad (37)$$

This expression describes the kinetic data of Olson *et al.* (34) which were obtained in a differential reactor and under conditions where $P_{SO_3} > K_PK_{Pt}$ (Fig. 13). Only C' was fitted.

To summarize, the experimental equa-

tions (6) and (11) are consistent with a Langmuir model for the dependence of surface oxygen activity on surface oxygen coverage. In Region 2 desorption of SO_3(Pt) is rate limiting and P_{SO_3} has no direct effect on the rate which is given by (34) as long as P_{SO_3} is not very close to $K_P K_{Pt}$. When it is, the reverse reaction (adsorption) gives the appearance of poisoning. In Region 3 equilibrium is established between surface and gaseous SO_3, oxygen chemisorption becomes rate limiting, and SO_3 has a poisoning effect on the forward reaction [Eq. (37)].

Silver and gold. The reciprocal relationship between P_{SO_2} and $a_{O_2(Pt)}^{1/2}$ observed during the SO_2 oxidation on Pt was interpreted in terms of establishment of the equilibrium described by Eq. (18).

By an identical argument Eq. (13) suggests establishment of the equilibrium

$$SO_2(g) + O(Ag) \rightleftarrows SO_3(Ag), \quad (38)$$

where again the chemical potential of chemisorbed SO_3 is a function of temperature only. Silver sulfate formation is ruled out since the ΔH for the reaction

$$Ag_2O + SO_2 + \tfrac{1}{2}O_2 \rightleftarrows Ag_2SO_4$$

is -92.23 kcal/mol compared with a ΔH of -47.5 kcal/mol derived from the temperature dependence of K_{Ag} [Eq. (13)]. By arguments similar to those used to derive Eq. (21) one obtains

$$\mu_{SO_3(Ag)} - \mu^\circ_{SO_3(g)} = 7.63RT - 12{,}560R. \quad (39)$$

It follows from Eq. (39) that ΔH and ΔS for SO_3 chemisorption on silver are given by $\Delta H_{SO_3(Ag)} = -24.9$ kcal/mol and $\Delta S_{SO_3(Ag)} = -15.1$ cal/mol K. The ΔS value satisfies all the criteria established by Boudart *et al.* (*35*) for entropy changes associated with chemisorption. The ΔH value, compared with the ΔH value of -12.3 kcal/mol for SO_3 chemisorption on Pt, provides an explanation for the noncatalytic nature of Ag for the SO_2 oxidation. Since desorption of SO_3 was found to be the rate-limiting step of the SO_2 oxidation on Pt when equilibrium (18) is established, SO_3 desorption from Ag must also be rate limiting when equilibrium (38) is established. The failure of Ag to act as a catalyst must result then from the high activation energy for SO_3 desorption ($\sim$24.9 kcal/mol) relative to that for SO_3 desorption from Pt ($\sim$12.3 kcal/mol).

Since within the temperature and gas phase composition range investigated the surface oxygen activity on gold is a function of P_{SO_2} and T only and does not depend on P_{SO_3}, it can be concluded that, as in the case of Pt and Ag, equilibration between surface and gas phase SO_3 is not established and SO_3 desorption is rate limiting. If one represents the surface equilibrium by

$$\Theta_{SO_2} \cdot \Theta_O = \frac{1}{K_s} \Theta_{SO_3}, \quad (40)$$

where Θ_{SO_2}, Θ_{SO_3}, and Θ_O are surface coverages and K_s is the surface reaction equilibrium constant, then Eq. (15) can be interpreted in terms of a Langmuir–Hinshelwood model. Within that framework the functional dependence of Θ_O on $a_{O_2(Au)}$ when equilibrium between surface and gas phase oxygen is not established is the same as the functional dependence of Θ_O on P_{O_2} when equilibrium is established. Further, assuming that (a) the activity of chemisorbed SO_3 is a function of temperature and is represented by $K_P K_{Au}$ (analogous to the expressions for Pt and Ag) so that

$$\mu_{SO_3(Au)} - \mu^\circ_{SO_3(g)} = RT \ln K_P K_{Au}; \quad (41)$$

and (b) that oxygen chemisorption is stronger than the chemisorption of SO_2 and SO_3, one obtains from Eq. (40):

$$\frac{K_{SO_2} K_O P_{SO_2} \cdot a_{O_2(Au)}^{1/2}}{(1 + K_O a_{O_2}^{1/2}{}_{(Au)})^2} = \frac{1}{K_s} \frac{K_{SO_3} K_P K_{Au}}{1 + K_O a_{O_2(Au)}^{1/2}}, \quad (42)$$

where K_{SO_2}, K_O, and K_{SO_3} are the corresponding adsorption coefficients. Since $K_{SO_2} \cdot K_O \cdot K_{SO_3}^{-1} \cdot K_s^{-1} = K_P$, one obtains Eq. (15). From Eqs. (16) and (41) it follows that ΔH and ΔS for SO_3 chemisorption on Au are -19.0 kcal/mol and -12.5 cal/mol K, respectively.

The values of $K_P K_{Au}$ which express the activity of SO_3 chemisorbed on gold fall between the values of $K_P K_{Pt}$ and $K_P K_{Ag}$ (Fig. 14), and since SO_3 desorption is rate limiting in all three cases, this provides an explanation for the weak catalytic properties of gold for the SO_2 oxidation. Thus the surface oxygen activity is an appropriate measure of catalytic activity of Pt, Au, and Ag for this reaction.

The oxygen activity and the exchange current reaction. The use of a_{O_2} as a measure of the catalytic activity of these metals is based on the assumption that ZrO_2 itself plays no role in the reaction. It is not a catalyst for the SO_2 oxidation (*30*) but does exhibit SO_2 adsorption at room temperature (*36*). If SO_2 can attack O^{2-} ions, the measured oxygen activity would differ from that of the gas phase but would be the same for all metals. This is not observed, strongly supporting the current interpretation that the measurement does not reflect the electrolyte characteristics and the reaction between gaseous SO_2 and O^{2-} cannot be the dominant exchange current reaction. If, however, the attack occurs at the three-phase boundary, a metal-specific oxygen activity would be observed which might not correspond to the true oxygen activity on the metal. This can be ruled out by the close correlation between the electrochemically measured oxygen activity and the observed global reaction kinetics on Pt.

That gaseous oxygen/electrode equilibration may not occur when a chemical reaction involving the gas phase proceeds at the electrode surface is a phenomenon known to electrochemists (*27*). It is usually described in terms of nonideal potential

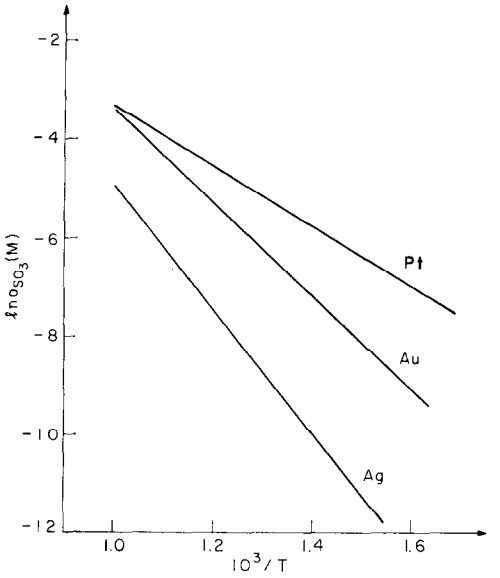

FIG. 14. Activity ($a_{SO_{3(M)}} = K_P K_M$) of SO_3 chemisorbed on Pt, Au, and Ag under conditions where SO_3 desorption is rate limiting.

behavior, the implication of nonideal being that the cell EMF does not satisfy Eq. (2), but is determined by intermediate products adsorbed at the electrode surface rather than by the primary gaseous species. In addition to this mechanism, which is the one adopted here, direct electrochemical processes between gas and electrolyte ions can also lead to nonideal behavior. Such processes lead to an alteration of the dominant exchange current reaction and have been partly invoked by Fleming (*21*) to describe the behavior of zirconia-based oxygen sensors used in the exhaust line of motor vehicles. No such processes need be invoked for the SO_2 oxidation, particularly since, as was noticed earlier, the attack of O^{2-} by gaseous SO_2 is very unlikely to be a dominant exchange current reaction.

The present results also establish the temperature and gas phase composition limits for the use of stabilized zirconia cells with Pt electrodes as an electrochemical sensor for the determination of P_{O_2} (Region 1), P_{SO_2} (Region 2), and the

P_{SO_3}/P_{SO_2} ratio (Region 3) in SO_2, SO_3, oxygen, inert gas mixtures.

SUMMARY

An electrochemical oxygen concentration cell utilizing a solid electrolyte (ZrO_2, Y_2O_3) with Pt, Ag, and Au electrodes, one of which functioned simultaneously as a catalyst, was used to measure the activity of oxygen on the metal during the catalytic oxidation of SO_2. It was observed that the equilibrium between gaseous and adsorbed oxygen could not be maintained and new equilibrium processes involving $SO_2(g)$ were found with Pt films. For sufficiently low P_{SO_3}, an equilibrium constant of the form $P_{SO_2} \times a_{O_2(Pt)}^{1/2} = K_{Pt}$ indicated the presence of a chemisorbed SO_3 phase with a chemical potential depending only on temperature. The stability of this phase, $SO_3(Pt)$, is limited. When P_{SO_3} exceeds some critical value, this equilibrium is replaced by another of the form $(P_{SO_3}/P_{SO_2}) = K_P \times a_{O_2(Pt)}^{1/2}$. Only for $P_{SO_2} \times P_{O_2}^{1/2} < K_{Pt}$ was O_2 equilibrium with the surface observed. These three stability regions result in three different kinetic regions. In the very low SO_2 pressure region where $SO_3(Pt)$ does not exist no kinetic data were taken, but where $SO_3(Pt)$ exists, the kinetics appear to be dominated by the desorption of $SO_3(Pt)$. The poisoning by SO_3 in this region is the result of a vapor saturation effect. When P_{SO_3} exceeds the critical value defined by the vapor pressure of $SO_3(Pt)$, $SO_3(Pt)$ is destroyed and the kinetics appear to be dominated by the rate of O_2 chemisorption. Poisoning by SO_3 in this region is a usual site-blocking process. With no assumptions other than global rate scaling the parameters deduced from this study describe precisely the data of Smith *et al.* (*34*) and represent a viable alternative to the oxygen equilibration model which had been employed to interpret them.

For Ag and Au films the formation of a chemisorbed SO_3 phase similar to Pt is observed and over the limited range of parameters investigated, SO_3 desorption appears to be rate-limiting step. The present results show that the difference in the catalytic activity of Pt, Au, and Ag for the SO_2 oxidation is not due to a qualitative difference in the ability of these metals to form an appropriate intermediate species, but results from a quantitative difference in the binding strength of product SO_3 to the surface.

The catalytic surface processes described above have complicated the understanding of electrochemical oxygen gas sensors but make possible a significant opportunity for a better understanding of heterogeneous catalytic oxidations on metals at the molecular level.

ACKNOWLEDGMENTS

This research was supported under NSF Grant GK 38727. Fellowship support from the E. H. Hooker Foundation to C.G.V. is gratefully acknowledged.

REFERENCES

1. Wagner, C., *Advan. Catal.* **21**, 323 (1970).
2. Bodenstein, M., and Fink, F., *Z. Phys. Chem.* **60**, 1 (1907).
3. Lewis, W. K., and Ries, E. D., *Ind. Eng. Chem.* **19**, 830 (1927).
4. Taylor, G. B., and Lenher, S., *Z. Phys. Chem.* **23**, 30 (1931).
5. Penyi, N. I., *J. Phys. Chem.* (*USSR*) **14**, 981 (1940).
6. Boreskov, G. K., *J. Phys. Chem.* (*USSR*) **19**, 535 (1945).
7. Boreskov, G. K., and Chesalova, V. S., *Zh. Fiz. Khim.* **30**, 2560 (1956).
8. Uyehara, O., and Watson, K. M., *Ind. Eng. Chem.* **35**, 541 (1943).
9. Hurt, D. M., *Ind. Eng. Chem.* **35**, 522 (1943).
10. Olson, R. W., Schuler, R. W., and Smith, J. M., *Chem. Eng. Prog.* **46**, 614 (1950).
11. Dartyan, O. K., and Ovchinnikova, E. N., *Dokl. Akad. Nauk. USSR* **104**, 857 (1955).
12. Atroshcenko, Tseitlin, and Toshinskii, *Ukr. Khim. Zh.* **37**, No. 3, 287 (1971).
13. Weychert, S., and Urbanek, A., *Int. Chem. Eng.* **9**, No. 3, 396 (1969).

14. Silva, A., Hudgins, R., and Silveston, P., *J. Catal.* **49**, 376 (1977).
15. Taylor, Kistiakowsky, and Perry, *J. Phys. Chem.* **34**, 799 (1930).
16. Bond, G. C., "Catalysis by Metals," p. 464. Academic Press, New York, 1962.
17. Ashmore, P. G., "Catalysis and Inhibition of Chemical Reactions," pp. 225–237. Butterworths, London, 1963.
18. Kiukkola, K., and Wagner, C., *J. Electrochem. Soc.* **104**, 379 (1957).
19. Burke, L., Rickert, H., and Steiner, R., *Z. Phys. Chem. NF* **74**, 146 (1971).
20. Weissbart, J., and Ruka, R., *Rev. Sci. Instrum.* **32**, 593 (1961).
21. Fleming, W., *J. Electrochem. Soc.* **124**, 21 (1977).
22. Weissbart, J., and Ruka, R., *J. Electrochem. Soc.* **109**, 723 (1962).
23. Etsel, T. H., and Flengas, S. N., *J. Electrochem. Soc.* **109**, 723 (1962).
24. Weissbart, J., Smart, W. H., and Wyderen, T., *Aerosp. Med.* **40**, 136 (1969).
25. Pancharatnam, S., Huggins, R. A., and Mason, D. M., *J. Electrochem. Soc.* **122**, 869 (1975).
26. Briggs, T. P., Hudgins, R. R., and Silveston, P. L., *Int. J. Mass Spectrom. Ion Phys.* **20**, 1 (1976).
27. Dietz, H., Haecker, W., and Jahnke, H., *in* "Advances in Eelctrochemistry and Electrochemical Engineering" (H. Gerischer and C. W. Tobias, Eds.), Vol. 10, p. 1. Wiley–Interscience, New York, 1977.
28. Kleitz, M., Fabry, P., and Schoule, E., *in* "Electrode Processes in Solid State Ionics" (M. Kleitz and J. Dupuy, Eds.), p. 1. Reidel, Dordrecht, 1976.
29. Weinberg, W. H., and Merrill, R. P., *Surface Sci.* **39**, 206 (1973).
30. Vayenas, C., Ph.D. thesis, University of Rochester, 1977.
31. Schmidt, M., and Siebert, W., "Comprehensive Inorganic Chemistry: The Chemistry of S." Pergamon, Long Island City, N.Y., 1975.
32. Tracy, T. C., *J. Chem. Phys.* **56**, 2736 (1972).
33. Madix, R., *Catal. Rev.* **15**, 293 (1977).
34. Smith, J. M., *in* "Chem. Eng. Kinetics," 2nd ed., p. 348. McGraw–Hill, New York, 1970.
35. Boudart, M., Mears, D. E., and Vannice, M. A., *Ind. Chim. Belg.* **32**, 281 (1967).
36. Shelef, M., private communication.